AD-A055 906 CALIFORNIA UNIV BERKELEY DEPT OF CHEMICAL ENGINEERING F/G 11/9
VISCOELASTIC PROPERTIES OF ENTANGLED POLYMER IV. BINARY BLENDS --ETC(U)
MAY 78 D SOONG, M SHEN, S D HONG N00014-75-C-0955
UNCLASSIFIED TR-20 NL

END
DATE FILMED
8-78
DDC

(9) Technical Report No. 20

(6) VISCOELASTIC PROPERTIES OF ENTANGLED POLYMER
IV. BINARY BLENDS OF MONODISPERSE HOMOPOLYMERS

(12)

by (15) (14) TR-20
NR014-75-C-0955

(10) D. Soong, and M. Shen
Department of Chemical Engineering
University of California
Berkeley, California 94720

and

S. D. Hong
Jet Propulsion Laboratory
Pasadena, California 91103

(11) 1 May 1978 (12) 37 p.

Technical Report to be published in
Journal of Rheology

Approved for public release: Distribution Unlimited

Prepared for
Office of Naval Research
800 North Quincy Street
Arlington, Virginia 22217

404 601

VISCOELASTIC PROPERTIES OF ENTANGLED POLYMERS.

IV. BINARY BLENDS OF MONODISPERSE HOMOPOLYMERS

by

D. Soong and M. Shen
Department of Chemical Engineering
University of California
Berkeley, California 94720

and

S. D. Hong
Jet Propulsion Laboratory
Pasadena, California 91103

ABSTRACT

In a previous publication from this laboratory, the Rouse-Bueche-Zimm molecular theory of viscoelasticity has been extended by using a transient network model to apply to monodisperse polymers with chain entanglements. Effects of the entanglements were modeled both by the enhanced frictional coefficients and by the additional elastic couplings resulting from the transient entanglement network. For binary blends consisting of two monodisperse polymers with different molecular weights, additional modifications are now required to predict their linear viscoelastic behavior. It is recognized that entanglements not only may form between chains of the same lengths, but also between those of different lengths. For the latter case, the longer chain will in fact have the frictional coefficient of the shorter chain at the point of entanglements. The frequency of such interactions is assumed to be proportional to the weight ratio of the respective component chains in the blend. Equations of motion are formulated for each component and solved numerically for the relaxation spectra. Linear viscoelastic parameters such as the dynamic

mechanical moduli, stress relaxation moduli, and zero shear viscosity can then be computed for the blends by linear summation of those of the components. The reduced steady state shear compliance of the blends can also be computed from knowledge of the component relaxation times. Results are found to be in excellent agreement with literature data on polystyrene, poly(dimethyl siloxane) and poly(methyl methacrylate).

INTRODUCTION

The molecular theory of viscoelasticity for isolated polymers expounded by Rouse (1), Bueche (2), and Zimm (3) has previously been extended by a number of workers (4-9) to predict the viscoelastic properties of bulk polymers with molecular weights exceeding their critical entanglement molecular weights, M_c. In recent series of publications from this laboratory (10-12), several models were considered which incorporate the effects of enhanced friction and elastic coupling of the entangled chains. The most successful, and intuitively most reasonable, model envisions the entangled systems as forming a three dimensional transient network (12). The predicted linear viscoelastic properties for monodisperse entangled polymers were found to be in excellent agreement with literature data for a number of systems.

Attempts to describe the viscoelastic properties of polymer blends from those of their known monodisperse fractions are motivated by its potential engineering applications to the mixed system. In addition, an understanding of the multitudinous interactions among the components may provide a possible means toward

predicting the viscoelastic properties of the polydisperse polymers. A number of workers invoked some empirical blending rules to obtain the relaxation spectra of mixtures from their constituents (13-18). However, polymer molecules should behave differently in a blend than in their pure state because of the interactions with the coexisting components of different chain lengths. The response and motion of the fractions must therefore be mutually affected by all the components present in the blend. The resulting relaxation spectra associated with any given component must be different in a blend from that in the pure, unmixed state. Merely mixing the unmodified relaxation spectra of the components to form the relaxation spectra for the blend without taking into account of the aforementioned mutual interactions between the components would be inadequate in describing the viscoelastic behavior of polymer blends.

In this work, we shall apply the transient network model (12) to binary blends by incorporating the effect of the co-existing components on chain dynamics. We are then able to obtain the modified relaxation times for each component. The linear viscoelastic properties of the blends are subsequently obtained by summing properties of the corresponding component calculated by the modified relaxation times.

THEORY

In a polymer blend made of monodisperse fractions whose molecular weights exceed the critical molecular weight, all the polymer molecules entangle with their surrounding neighbors to constitute a three dimensional network structure. The

difference between this kind of network and the ones formed by the monodisperse components alone is that in the blend entanglements may be formed from chains of different lengths. The chain dynamics in these systems may be expected to differ significantly from the monodisperse polymers.

Following the transient network model for monodisperse polymers, the equation of motion for an unentangled bead B is (12)

$$\dot{x}_k = V^s_{x_k} - \frac{kT}{f_B}\frac{\partial \ln\psi}{\partial x_k} - \frac{3kT}{f_B\langle b_o^2\rangle}(-x_{k+1} + 2x_k - x_{k-1}) \qquad (1)$$

where $k\neq 0,N$, N is the total number of beads in the chain and $\langle b_o^2\rangle$ is the mean square end-to-end distance of a statistical segment, x_k and $\dot{x}_k$ are respectively the x-component of the coordinates and velocity of the kth bead, $V^s_{x_k}$ is the velocity of the medium surrounding the kth bead, f_B is the frictional coefficient of the unentangled bead, and ψ is the segmental distribution function.

For an entangled bead A, the corresponding equation assumes the following form:

$$\dot{x}_j = V^s_{x_j} - \frac{kT}{f_{A_j}}\frac{\partial \ln\psi}{\partial x_j} - \frac{3kT}{f_{A_j}\langle b_o^2\rangle}(-x_{j+1} + 2x_j - x_{j-1})$$

$$- \frac{3kT}{f_{A_j}\langle b_o^2\rangle}\sum_{i=1}^{N_e}\varepsilon_{ji}\,(x_j - x_i^I) \qquad (2)$$

where $\varepsilon_{ji} = \dfrac{\alpha}{|j-i|}$ (3)

and $j \neq i \neq k$, f_{A_j} is the frictional coefficient of the entangled bead at x_j. The fourth term on the right-hand side of Eq. 2 accounts for the elastic coupling forces acting between all pairs of N_e entangled beads (12). They are inversely proportional to the interbead distance as shown in Eq. 3. α is a parameter to account for the fact that the entanglement is not as effective as a permanent crosslink in transmitting force, since entangled chains can slip by each other. Its value is between 0 and 1. Throughout the calculations, the enhanced frictional coefficient f_{A_j} is assumed to have the high-friction-inside distribution, i.e., entangled beads near the chain middle have higher frictional coefficients than the ones at the chain ends. This type of distribution is not only intuitively reasonable, but also has been found to fit the experimental data very well for monodisperse polymers (12).

In a polymer blend made of monodisperse fractions having different molecular weights, further modifications of the equation of motion must be imposed. For simplicity the following derivation will be given for a binary blend. Extension to multiple blends can be similarly analyzed. We begin by assuming that the blend is a homogeneous one, and shows no evidence of microphase separation. This assumption may be considered valid for the type of blends under consideration , i.e., blends of different molecular weight fractions of the same polymer. The absence of heterogeneous domain formation is one of the basic tenets of the RBZ model. For a given component chain in a binary blend, it can form entanglements with another chain of the same length or that of a different length. The probability of entanglement formation

between chains belonging to different components and those belonging to the same component in a well-mixed blend is expected to be proportional to the abundnace of the components if we assume that the tendencies for chain segments to entangle are the same irrespective of the chain lengths as long as they exceed the critical molecular weight. The ratio of inter-component and intra-component entanglements is therefore dependent upon the composition of the blends, being proportional to the weight ratio of the components according to our assumption. Here, inter-component entanglement is defined as entanglement formed between two beads belonging to chains of different lengths, and intra-component entanglement corresponds to that between chains of the same length.

Entanglement formation restricts chain motion of both chains at the entangled point. The extent of retardation is the same for both chains. At an inter-component entanglement, motion of the longer chain is facilitated because it is entwined with a shorter chain. This serves to reduce the frictional coefficient of the longer molecule at the inter-component entanglement point. In other words, the longer molecule now has the smaller frictional coefficient previously associated with the shorter molecule while the frictional coefficient of the shorter molecule remains unchanged. This is a reasonable assumption, since the frictional coefficients must be the same for both beads from either chain at the point of entanglement. Because of the greater mobility of the shorter chain, the entangled beads on both chains now are less restrained. We can now write the equation of motion for such a system in matrix notation as:

$$\dot{\underset{\sim}{X}} = \underset{\sim}{V}^{s}_{x} - D_B \underset{\sim}{D}^{-1} \frac{\partial \ln \psi}{\partial \underset{\sim}{X}} - \sigma_B \underset{\sim}{D}^{-1} \underset{\sim}{Z}_e \underset{\sim}{X} \qquad (4)$$

where $\dot{\underset{\sim}{X}}$ and $\underset{\sim}{X}$ are column vectors of velocity and position of the beads respectively, $\underset{\sim}{V}^{s}_{x}$ is the x-component of the velocity of the surrounding medium, $D_B = \frac{kT}{f_B}$ is the diffusion coefficient, $\sigma_B = \frac{3kT}{\langle b_o^2 \rangle f_B}$ and $\underset{\sim}{D}^{-1}$

is the inverse of the diagonal matrix

$\underset{\sim}{D}$:

$$\underset{\sim}{D} = \begin{bmatrix} 1\left(\delta_2^1\right) & & & & & \\ & 1\left(\delta_4^2\right) & & & & \\ & & 1 & & & \\ & & & \left(\delta_j^I\right)_1 & & \\ & & & & \ddots & \\ & & & & & 1 \end{bmatrix} \qquad (5)$$

where $\delta_j^I = \dfrac{f_{A_j}^I}{f_B}$ and $f_{A_j}^I$ now is the modified high-friction-inside distribution of the enhanced frictional coefficients. For a given component in a binary blend, a number of the δ_j^I's are chosen randomly to be replaced by those corresponding to the other component so as to represent inter-component entanglements. The frequency of such exchange is proportional to the amount of the latter component present in the blend. $\underset{\sim}{Z}_e$ is the modified version of the nearest-neighbor matrix for an entangled polymer. As an example, the form of $\underset{\sim}{Z}_e$ for a chain with alternating entangled and unentangled beads is:

$$\underset{\sim}{Z}_e = \begin{bmatrix} 1 & -1 & 0 & 0 & 0 & 0 & \cdots \\ -1 & 2+\gamma_2 & -1 & -\varepsilon_{24} & 0 & -\varepsilon_{26} & \cdots \\ 0 & -1 & 2 & -1 & 0 & 0 & \cdots \\ 0 & -\varepsilon_{42} & -1 & 2+\gamma_4 & -1 & -\varepsilon_{46} & \cdots \\ 0 & 0 & 0 & -1 & 2 & -1 & \cdots \\ - & - & - & - & - & - & - \\ - & - & - & - & - & - & - \end{bmatrix} \qquad (6)$$

where $$\gamma_i = \sum_{\substack{j=1 \\ j \neq (i-1),\ i,\ (i+1)}}^{N_e} \varepsilon_{ij} \qquad (7)$$

We can write a matrix equation for each component in the blend and, upon solving it, obtain the relaxation times of the component given by

$$\tau_p = \frac{1}{2\sigma_B \gamma_p} \qquad (8)$$

where γ_p is the p-th eigenvalue of $\underset{\sim}{D}^{-1}\ \underset{\sim}{Z}_e$. The interactions between components have been incorporated into the matrix equations, the resulting component relaxation times are therefore the modified relaxation times. The degree of modification depends on the composition as explained before, the calculated relaxation times for the components hold true only for the particular composition for which the calculations have been carried out. The relaxation times for the same component polymer chain vary with the composition of the blend.

Further refinement must be introduced to our basic theoretical framework upon recognition of the fact that these inter-component entanglements can take place at different positions along a given chain. Since we have adopted the high-friction-inside distribution as our basis, replacing frictional coefficients means utilizing a different set of numbers when the entanglements occur at different positions along both chains. Two approaches can be employed to tackle this problem.

The first method is to select randomly the beads whose frictional coefficients are to be changed, and then calculate the relaxation times from which the various viscoelastic properties can be found. The whole procedure is repeated many times and the resulting viscoelastic properties are averaged in an attempt to produce a good representation of the system. This is the "post-averaging" method.

The second method assumes that all the entangled beads along a given chain have equal probability of forming intercomponent entanglements with any of the entangled beads of the other components. As an example, consider a 50/50 weight percent binary blend. A given entangled bead on a given chain is involved in inter-component entanglement half of the time and intra-component entanglement the other half of the time over a long period of observation. Equivalently, for a mixture containing a huge number of molecules, for the same entangled point, half of the molecules are involved in inter-component entanglement formation and the other half in intra-component entanglement at any given instant. We can therefore "pre-average" the frictional coefficients and use the resulting average to set up the matrix equations as a representation of the collection of chains in the mixture.

Suppose that our example of a 50/50 (by weight) binary blend is made of components having 10 and 20 entanglements respectively. Based on the "equal entangling tendency" assumption, five out of the ten entanglements in the shorter component are involved in inter-component entanglements on the average, and

ten out of twenty for the longer component. The post-averaging method randomly selects ten of the δ_j^I's in the D matrix corresponding to the longer component and replaces them by those corresponding to the shorter component. The inserted values are also picked randomly from the δ_j^I's of the shorter components. The resulting viscoelastic parameters are calculated and stored in the memory bank, and at the end of the computation, the stored data are averaged to obtain the "post-averaged" properties.

If the random selection process is repeated many times, eventually any entanglement along the longer chain will assume its original frictional coefficient half of the times, while for the other half of the times it will have frictional coefficients belonging to the shorter component. Since we adopted the high-friction-inside distribution (12), i.e. $f_{A_j}^I = I^4$, where I is the position of the entanglement counted from chain ends, the proposed preaveraging method assigns the frictional coefficients according to the following rule:

$$f_{A_j} = W_j I^4 + W_k \sum_{L=1}^{N_{e_k}/2} L^4/(N_{e_k}/2)$$

when N_{e_k} is even; and

$$f_{A_j} = W_j I^4 + W_k [(N_{e_k}/2 + 1)^4 + 2\cdot(\sum_{L=1}^{N_{e_k}/2} L^4)] /N_{e_k}$$

when N_{e_k} is odd. In eqs. 9 and 10, W_j is the weight fraction and N_{e_j} is the number of entanglements of the longer component while subscript k refers to the shorter component in the blend. Eq. 9 ensures that the distribution is still high-friction inside while the effect of inter-component interactions is adequately taken into account.

For our example of a 50/50 blend, equation 9 is just:

$$f^{I}_{A_2} = 0.5\ (I^4) + 0.5 \sum_{L=1}^{10} \frac{L^4}{10} \qquad (11)$$

Solution of the post-averaging method is time-consuming and expensive in the cost of computations. One case has been tried and was found to approach the pre-averaging result as the number of reiteration of the random selection process increases. The pre-averaging method is thus chosen for the subsequent calculations.

Once the modified relaxation times are found, they can be used to calculate all the linear viscoelastic properties such as relaxation modulus, dynamic moduli, steady-state shear compliance and zero-shear viscosity by the well-known relations (10). The blend properties, except for the steady-state shear compliance, are just the linear sums of the corresponding properties of components because the relaxation times for each component are obtained from the already modified matrix equation to meet conditions existing at the particular composition considered. The steady-state shear compliance of the blend is obtained from the resulting relaxation times of the components by the appropriate equation to be shown later.

RESULTS AND DISCUSSION

In comparing the theoretical prediction with experimental data, one of the computed curves was shifted in coordinates until the terminal regions overlapped with data. All subsequent curves were not adjusted further once the fitting parameters have been chosen. The dynamic storage and loss shear moduli were computed by:

$$G'(\omega) = \frac{1}{N_e} \sum_p \frac{\omega^2 \tau_p^2}{1+\omega^2 \tau_p^2} \tag{12}$$

$$G''(\omega) = \frac{1}{N_e} \sum_p \frac{\omega \tau_p}{1+\omega^2 \tau_p^2} \tag{13}$$

Figure 1 compares the theoretical results with data on polystyrene blends. The solid curves are the computed curves. The symbols represent experimental data by Onogi et al. (19). To calculate the number of entanglements for a given monodisperse system (N_e), M_e is assumed to be 1.7×10^4 (10-12). The two curves on the outside are for the pure components of molecular weights of 5.9×10^4 and 6.16×10^5 respectively. We can see that the experimental data on the shorter component have not been accurately predicted. The reason is that the equivalent number of entanglements for this component should be about 3.5. However, the computer program can only calculate chains with integral number of entanglements and we are forced to use $N_e = 3$. The middle curve is a 50/50 (by weight) blend of the two components. The two-plateau tendency in the rubbery region of the dynamic storage moduli is successfully predicted.

In addition, the corresponding maximum near log $\omega = 0$ is also in excellent agreement with data. These phenomena are frequently observed for binary blends of two components having very different molecular weights. Fig. 2 shows results on another set of polystyrene binary blends by the same authors (19). The blends are 20/80, 40/60, 60/40, 80/20 by weight. Here the shorter component has a molecular weight corresponding to 2.5 entanglements. It is assumed to have 2 entanglements in our calculations. Agreement between theory and experiment is again very good.

Figure 3 compares the calculated curves with a set of dynamic mechanical data on blends of poly(methyl methacrylate) of molecular weights 4.1×10^3 and 1.74×10^4. The blends as indicated by the middle curves are 90/10, 80/20, 60/40, 30/70 percent by weight, the first number in the pair of numbers is the weight fraction pertaining to the lighter component. M_e for PMMA is assumed to be 7,000 (21). Agreement between theory and experiments is good except that the experimental data exhibit a more gradual terminal region, possibly due to its broader heterogeneity index (H.I. = 1.25).

The stress relaxation moduli calculated by the well known relation

$$E_R = \frac{1}{N_e} \sum_p e^{-t/\tau_p} \qquad (14)$$

are shown in Figure 4. Also given are the experimental data of Murakami and Ono (23) for monodisperse polystyrene fractions

with molecular weights of 1.87×10^5 and 5.83×10^5, as well as their 72/25 and 50/50 blends. The agreement between theory and experiment is good, except that the small second plateaus were not apparent in the predicted curves.

To compute the steady-state shear compliance, we recall that by definition

$$J_e^0 = NkT\Sigma\tau_i^2/(NkT\Sigma\tau_i)^2 \tag{15}$$

for a monodisperse polymer. For a binary blend, then

$$J_e^0 = \frac{N_1\Sigma\tau_i^2 + N_2\Sigma\tau_j^2}{RT(N_1\Sigma\tau_i + N_2\Sigma\tau_j)^2} \tag{16}$$

where τ_i's and τ_j's are the relaxation times of components 1 and 2 respectively, and N_1, N_2 are numbers of molecules of components 1 and 2 per unit volume. *In other words,*

$$J_e^0 = \frac{f_1\Sigma\tau_i^2 + f_2\Sigma\tau_j^2}{NRT(f_1\Sigma\tau_i + f_2\Sigma\tau_j)^2} \tag{17}$$

where f_1 and f_2 are mole fractions of components 1 and 2, i.e., $f_1 = \frac{W_1/M_1}{W_1/M_1+W_2/M_2}$ and $f_2 = 1-f_1$. The reduced steady-state shear compliance for a binary blend is thus

$$J_{eR} = \frac{f_1\Sigma\tau_i^2 + f_2\Sigma\tau_j^2}{(f_1\Sigma\tau_i + f_2\Sigma\tau_j)^2} \tag{18}$$

or

$$J_{eR} = \frac{\left(\frac{W_1}{M_1}\Sigma\tau_i^2 + \frac{W_2}{M_2}\Sigma\tau_j^2\right)\left(\frac{W_1}{M_1} + \frac{W_2}{M_2}\right)}{\left(\frac{W_1}{M_1}\Sigma\tau_i + \frac{W_2}{M_2}\Sigma\tau_j\right)^2} \tag{19}$$

Figure 5 shows the Log J_{eR} - W_2 data for three sets of binary blends of polystyrene. In addition to the data of Onogi (19) and Akovali (22), the more recent data of Porter and Prest (24) are also included. Both the data of Onogi and those of Porter and Prest show pronounced maxima, and are in fairly good agreement with our computed curves. The molecular weights in the binary blend of Onogi are 4.69×10^4, 1.67×10^5 and those of Porter/Prest are 9.72×10^4, 4.11×10^5. The molecular weights in the Akovali blend, on the other hand, are 1.25×10^5, 2.67×10^5. The molecular weight ratio is much lower than those in the former two blends. The J_{eR} now exhibit a much gentler maximum when plotted against W_2. The computed curves are still in reasonable agreement with the data, although the predicted maximum is sharper. Of course, if the molecular weight ratios in the binary blends decreases further toward unity, then a horizontal straight line would eventually be reached (a monodisperse system). Thus the trend is consistent with expectation. In Figure 6 we compare similar data of poly(methyl methacrylate), which are seen to be in excellent agreement with the theoretical curve.

The zero-shear viscosity can be computed from the relaxation spectra by

$$\eta_o = \frac{1}{N_e} \sum_p \tau_p \qquad (20)$$

The computed values are then plotted in Figure 7 against the weight average molecular weight of the blends containing different amounts of the two component monodisperse polystyrene fractions. The predicted curve is a straight line with a slope of 3.70, which is in good agreement with the experimental data of polystyrene represented by the circles (20).

The variation of the blend viscosity as a function of composition is an important engineering property and also a good criterion for testing our theory. Friedman and Porter (23) reviewed an exhaustive list of mixing rules, and compared them with experimental data. Following their convention, we plot in Figure 8 the viscosities of binary polystyrene blends against the weight fraction of the heavier component. The circles are experimental data (19) and the solid curves are the theoretical predictions. The numbers in the parenthesis give the equivalent entanglement bead number for the two components from which the blends are made of. Agreement between theory and experiments is seen to be excellent. Figures 9 and 10 show similar plots for two other polymer systems, i.e., poly(methyl methacrylate)(21) and poly(dimethyl siloxane) (26). Agreement is again very good.

For the cases examined above, all the viscosity - composition c curves concave downwards. However, the polystyrene blends studied by Akovali (22) revealed a somewhat sigmoidally-shaped curve. The only significant difference between this blend and the others is that the two components have a much smaller chain length difference in the former (Figure 11) than in the latter (Figures 8-10). Interestingly this trend is predicted by our theory (Figure 11). To further scrutinize the effect of chain length differences between components on the shape of the viscosity-composition curves, we show in Figure 12 the computed curves for a series of binary blends with varying chain-length differences. We note that if the lengths of the two components are not significantly different (up to a factor of two), the curves are sigmoidal. The theory in fact predicts a minimum

in viscosity if the chains are of comparable lengths, which has not been experimentally verified. The concave downward appearance, on the other hand, will be observed for components whose chain lengths differ more than a factor of two.

In conclusion, we can state that the transient network model is successful in predicting the linear viscoelastic behavior of monodisperse polymers (12) as well as their binary blends. The important feature of the model for blends is that it is not sufficient to just use some kind of mixing rules for the pure components alone. Simple intuitive reflection of the binary system will indicate that the cross entanglements between chains of different lengths must also be taken into account. The good agreement between the theoretical predictions and the literature data appears to vindicate the validity of this model.

ACKNOWLEDGEMENT

This work was supported by the Union Carbide Corporation and by the Office of Naval Research at the University of California and by the National Aeronautics and Space Administration at the Jet Propulsion Laboratory under contract #NAS7-100.

1. P. E. Rouse, J. Chem. Phys., 21, 1272 (1953).
2. F. Bueche, J. Chem. Phys., 22, 603 (1954).
3. B. Zimm, J. Chem. Phys., 24, 269 (1956).

4. F. Bueche, J. Chem. Phys., 20, 1959 (1952); ibid., 25, 599 (1956).

5. A. J. Chompff and J. A. Duiser, J. Chem. Phys., 45, 1505 (1966); ibid., 48, 235 (1968).

6. G. V. Vinogradov, V. H. Pokrovsky and Yu. G. Yanovsky, Rheol. Acta, 11, 258 (1972).

7. P. G. De Gennes, J. Chem. Phys., 55, 572 (1971).

8. W. W. Graessley, J. Chem. Phys., 47, 1942 (1967); ibid. 54, 5143 (1971).

9. W. C. Forsman and H. S. Grand, Macromol., 5, 289 (1972).

10. D. R. Hansen, M. C. Williams and M. Shen, Macromol., 9, 345 (1976).

11. S. D. Hong, D. R. Hansen, M. C. Williams and M. Shen, J. Polymer Sci.-Phys. Ed., 15, 1869 (1977).

12. S. D. Hong, D. Soong and M. Shen, J. Appl. Phys., 48, 4019 (1977).

13. H. Fujita and K. Ninomiya, J. Polymer Sci. 24, 233 (1957).

14. K. Ninomiya and J. D. Ferry, J. Colloid Sci. 18, 421, (1963).

15. D. C. Bogue, T. Masuda, Y. Einaga and S. Onogi, Polymer J. 1, 563 (1970).

16. W. W. Graessley, J. Chem. Phys. 54. 5143 (1971).

17. E. Menefee, J. Appl. Polymer Sci. 16, 2215 (1972).

18. M. Kurata, K. Osake and Y. Einaga, J. Polymer Sci. 12, 849 (1974).

19. T. Masuda, K. Kitagawa, T. Inoue and S. Onogi, Macromolecules 3, 116 (1970).

20. S. Onogi, T. Masuda, N. Toda and K. Koga, Polymer J., 1, 542 (1970).

21. R. S. Porter and J. F. Johnson, Chem. Revs., 66, 1 (1966).

22. G. Akovali, J. Polymer Sci. A-2, 5, 875 (1967).

23. K. Murakami and K. Ono, J. Polymer Sci., B10, 593 (1972).

24. W. M. Prest, Jr., and R. S. Porter, Polymer J. 4, 154 (1973).

25. E. M. Friedman and R. S. Porter, Trans. Soc. Rheo., 19, 493 (1975).

26. W. M. Prest, Jr., J. Polymer Sci., A-2, 8, 1897 (1970).

Table 1: Parameters Used in the Calculations and the Resulting J_{eR} and η_o.

Polymer	N+1	Ne	δ_j^I	α	J_{eR}	η_o
Polystyrene	7	3	I^4	0.2	0.333	0.972
	50/50 blend		"	"	-	1.92×10^3
	69	34	"	"	0.101	7.69×10^3
Polystyrene	7	2	I^4	0.2	0.409	0.508
	80/20 blend		"	"	-	3.52
	60/40 "		"	"	-	1.13×10
	40/60 "		"	"	-	2.37×10
	20/50 "		"	"	-	4.09×10
	21	10	"	"	0.269	6.29×10
Polystyrene	23	11	I^4	0.2	-	$8.50 \times 10_2$
	75/25 blend		"	"	-	4.71×10^2
	50/50 "		"	"	-	1.70×10^3
	69	34	"	"	-	6.71×10^3
Polystyrene	7	2	I^4	0.2	0.402	0.499
	90/10 blend		"	"	3.759	1.09
	80/20 "		"	"	3.824	2.82
	70/30 "		"	"	2.842	5.66
	60/40 "		"	"	2.073	9.62
	40/60 "		"	"	1.115	2.10×10
	20/80 "		"	"	0.591	3.68×10
	21	10	"	"	0.265	5.72×10
Polystyrene	15	7	I^4	0.2	0.336	1.52×10
	90/10 blend		"	"	0.828	1.74×10
	80/20 "		"	"	1.023	2.51×10
	70/30 "		"	"	0.871	3.83×10
	60/40 "		"	"	0.692	$5.67 \times 10_2$
	40/60 "		"	"	0.445	1.10×10^2
	20/80 "		"	"	0.291	1.85×10^2
	31	15	"	"	0.193	2.82×10^2
Polystyrene	13	6	I^4	0.2	0.396	8.4
	90/10 blend		"	"	2.313	2.58×10
	80/20 "		"	"	1.808	$7.76 \times 10_2$
	70/30 "		"	"	1.246	1.64×10^2
	60/40 "		"	"	0.874	2.85×10^2
	40/60 "		"	"	0.474	6.27×10^2
	20/80 "		"	"	0.261	1.11×10^3
	49	24	"	"	0.131	1.73×10^3

Table 1 (cont'd)

Poly(methyl-Methacrylate)	13	6	I^4	0.1	0.410	1.04×10
	90/10	blend	"	"	1.369	4.03×10
	80/20	"	"	"	2.143	1.29×10^2
	70/30	"	"	"	1.428	2.76×10^2
	60/40	"	"	"	0.994	4.82×10^2
	40/80	"	"	"	0.532	1.07×10^3
	20/80	"	"	"	0.289	1.90×10^3
	51	25	"	"	0.127	2.05×10^3
Poly(dimethyl-Siloxane)	7	3	I^4	0.2	-	0.972
	80/20	blend	"	"	-	1.02×10^2
	60/40	"	"	"	-	6.61×10^2
	40/20	"	"	"	-	2.44×10^3
	20/80	"	"	"	-	6.72×10^3
	79	39	"	"	-	9.75×10^3

CAPTIONS OF THE FIGURES

Figure 1. Plots of dynamic storage moduli $G'(\omega)$ and loss moduli $G''(\omega)$ vs frequency for polystyrene. The solid curves are computed curves. The symbols are experimental data (19). The two outer curves are for the pure components. The numerals at the bottom of the curves indicate the numbers of entangled beads. The curve in the middle (triangles) is a 50/50 (by weight) blend.

Figure 2. Plots of dynamic storage moduli $G'(\omega)$ and loss moduli $G''(\omega)$ vs frequency for polystyrene. The solid curves are computed curves. The symbols are experimental data (19). The two outer curves are for the pure components. The numerals at the bottom of the curves indicate the numbers of entangled beads. The curves between those for pure components are for 20/80, 40/60, 60/40, 80/20 (by weight) blends.

Figure 3. Plots of dynamic storage moduli $G'(\omega)$ and loss moduli $G''(\omega)$ vs frequency for poly(methyl methacrylate). The solid curves are computed curves. The symbols are the experimental data (20). The outer two curves are the pure components. The numerals at the bottom of the curves indicate the numbers of entangled beads. The curves between those of the pure components are for 90/10, 80/20, 60/40, 30/70 (by weight) blends.

Figure 4. Stress relaxation moduli for polystyrene. The solid curves are computed curves. The symbols are experimental data (22). The two outer curves are for the pure components. The ones between the pure component curves are for 75/25, 50/50 (by weight) blends.

Figure 5. Log-log plot of the reduced steady-state shear compliance of polystyrene vs weight fraction of the heavier component. Triangles, circles and squares are experimental data by Porter (26), Onogi (19) and Akovali (22) respectively. Curves were all computed by theory.

Figure 6. Log-log plots of the reduced steady-state shear compliance of poly(methyl methacrylate) vs. weight fraction of the heavier component. Circles are data of Onogi (20). The curve was calculated by theory.

Figure 7. Log-log plots of zero-shear-rate viscosity vs molecular weight. The lines were the computed curves. The circles are the experimental data (19) for pure polystyrene components and blends, all of which fall on the same straight line with a slope of 3.7. The triangles are data on poly(methyl methacrylates) (20).

Figure 8. Zero-shear viscosities of two polystyrene binary blend systems as a function of the weight fraction of the heavier component. Circles are experimental data of Onogi (19). Solid curves are theoretical predictions.

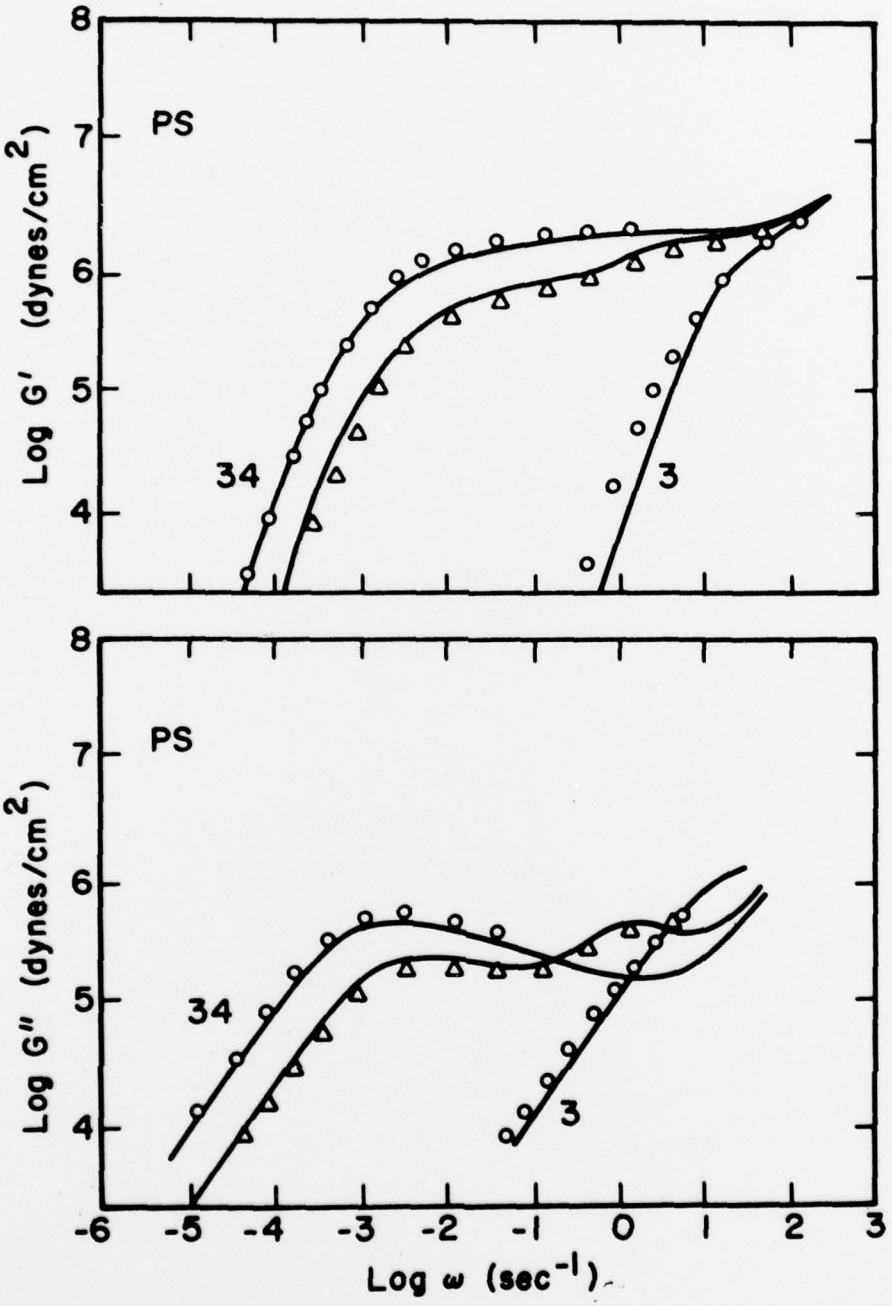
PS
Log G' (dynes/cm^2)
34
3
PS
Log G'' (dynes/cm^2)
34
3
Log ω (sec^{-1})

Figure 9. Zero-shear viscosities of poly(methyl methacrylate) binary blends as a function of the weight fraction of the heavier component. Circles are experimental data of Onogi (21). Solid curves are theoretical predictions.

Figure 10. Zero-shear viscosities of poly(dimethyl siloxane) binary blends as a function of the weight fraction of the heavier component. Circles are experimental data of Prest (25). Solid curves are theoretical predictions.

Figure 11. Zero-shear viscosities of polystyrene binary blends as a function of the weight fraction of the heavier component. Circles are experimental data of Akovali (22). Solid curves are theoretical predictions.

Figure 12. Zero-shear viscosities of binary blends for five different systems with different molecular weight ratios between the two constituent components. The curves are all calculated from the theory.

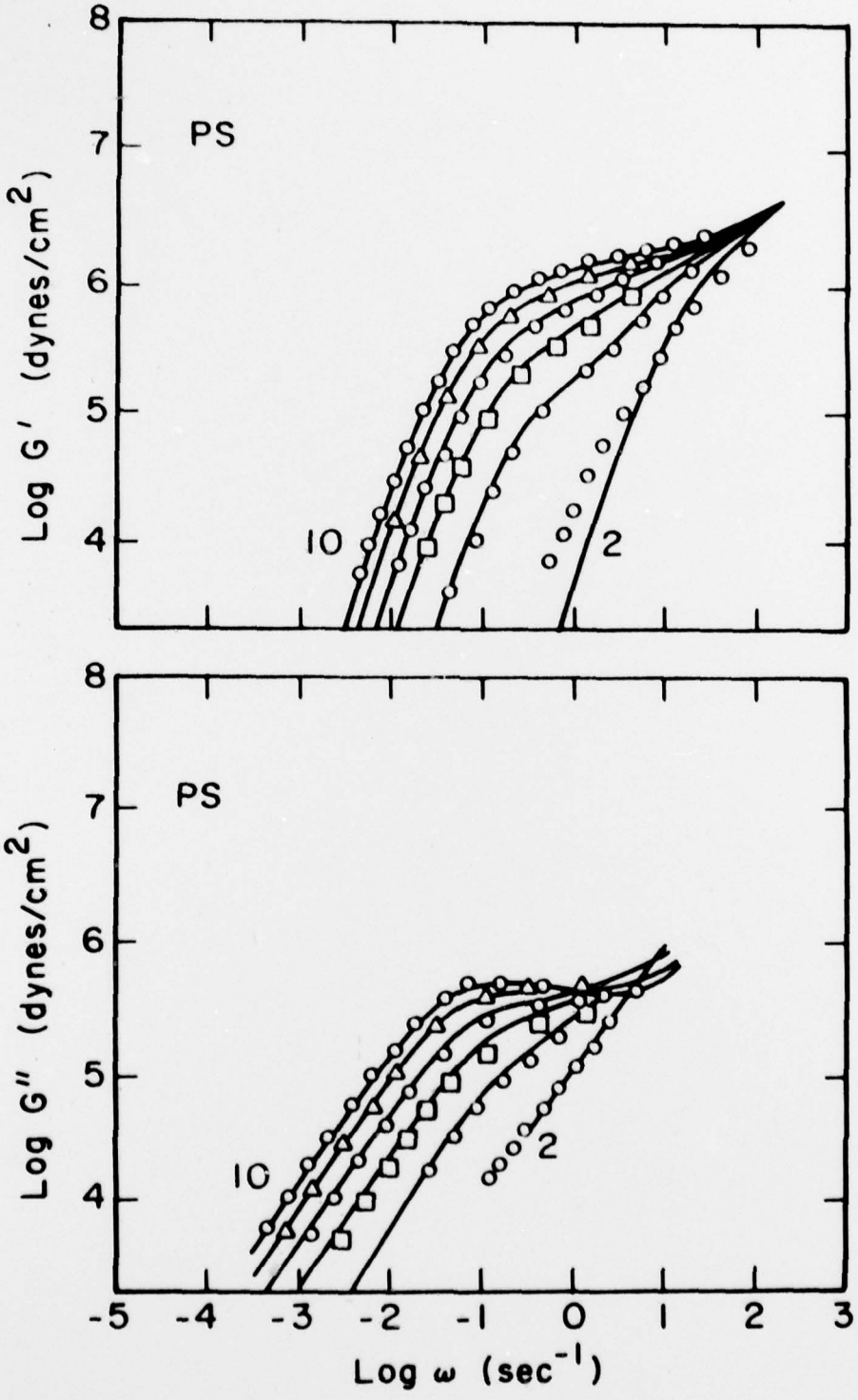
PS
Log G' (dynes/cm^2)
10
2
PS
Log G'' (dynes/cm^2)
10
2
Log ω (sec^{-1})

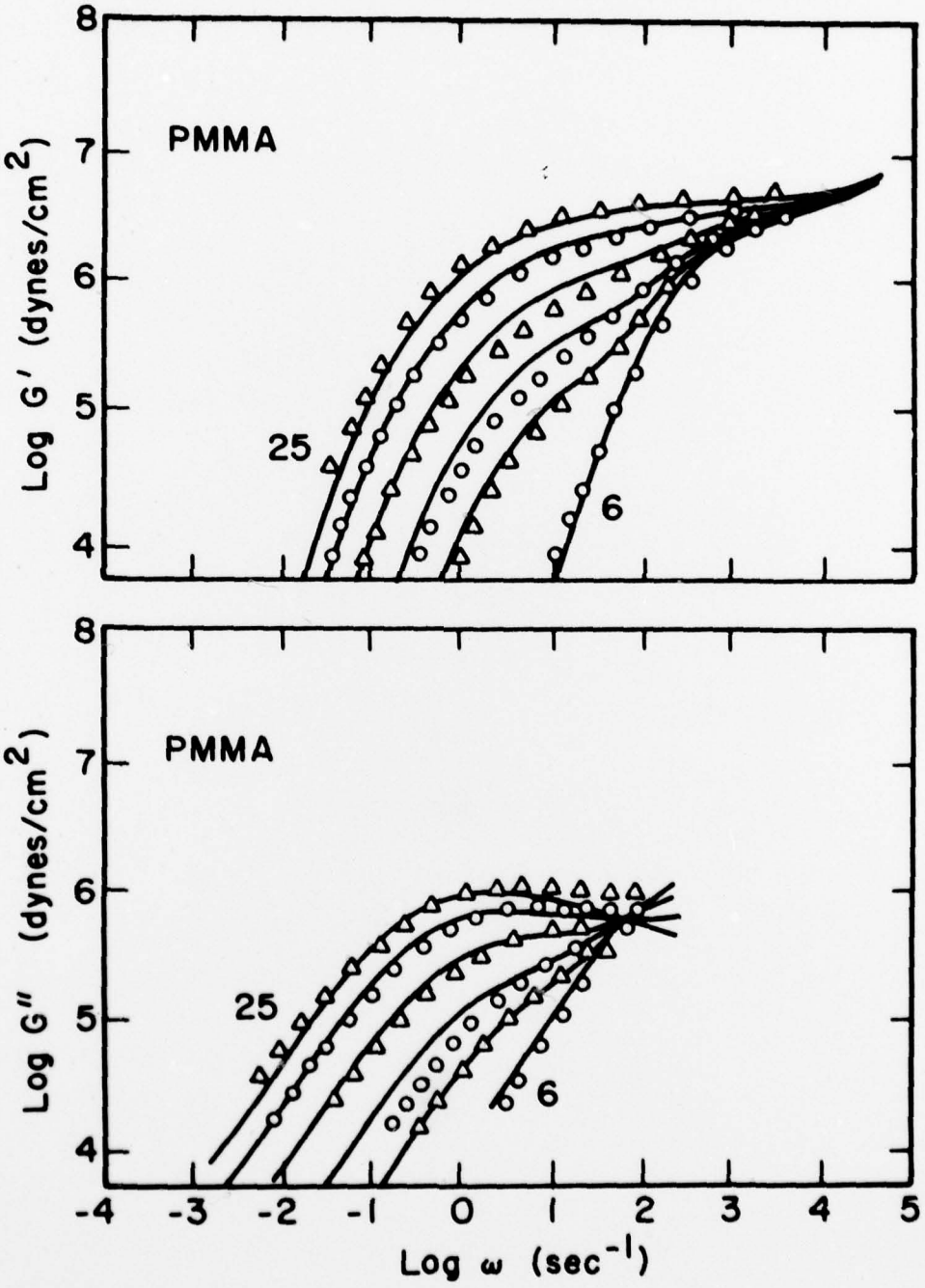
PMMA
Log G' (dynes/cm^2)
25
6
PMMA
Log G'' (dynes/cm^2)
25
6
Log ω (sec^{-1})

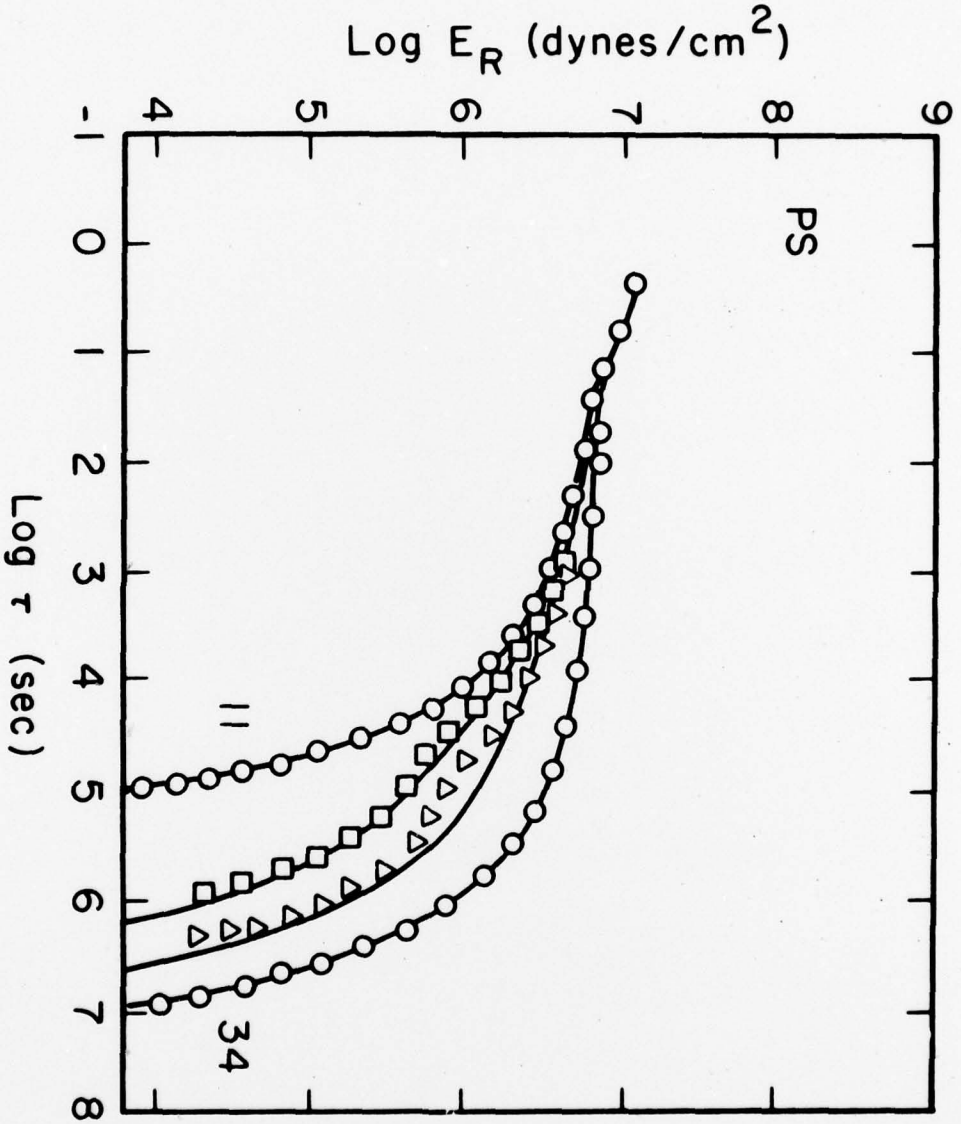
Log E_R (dynes/cm^2)
4
5
6
7
8
9
-1
0
1
2
3
4
5
6
7
8
Log τ (sec)
PS
11
34

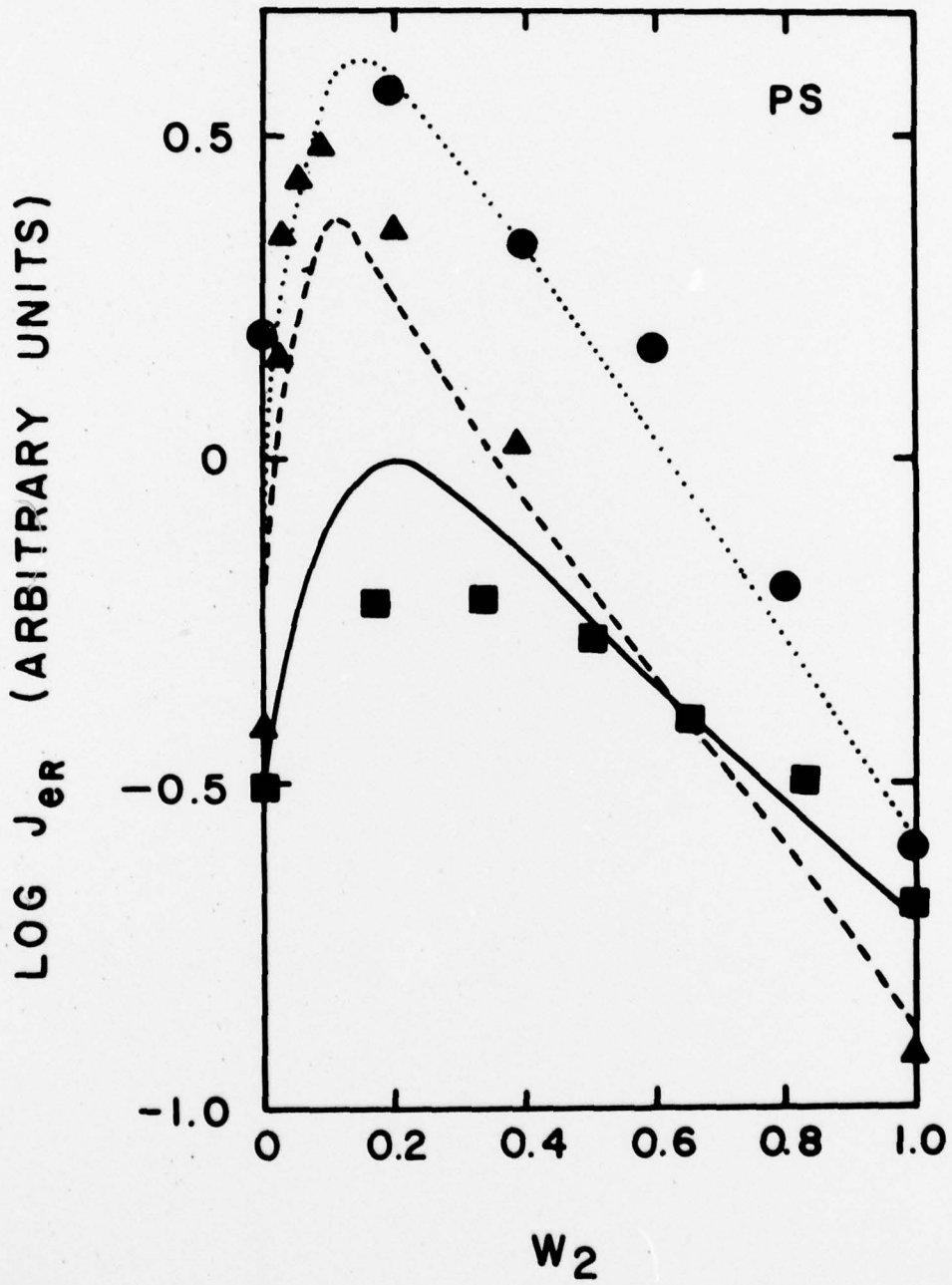
PS
0.5
0
−0.5
−1.0
0
0.2
0.4
0.6
0.8
1.0
LOG J_{eR} (ARBITRARY UNITS)
W_2

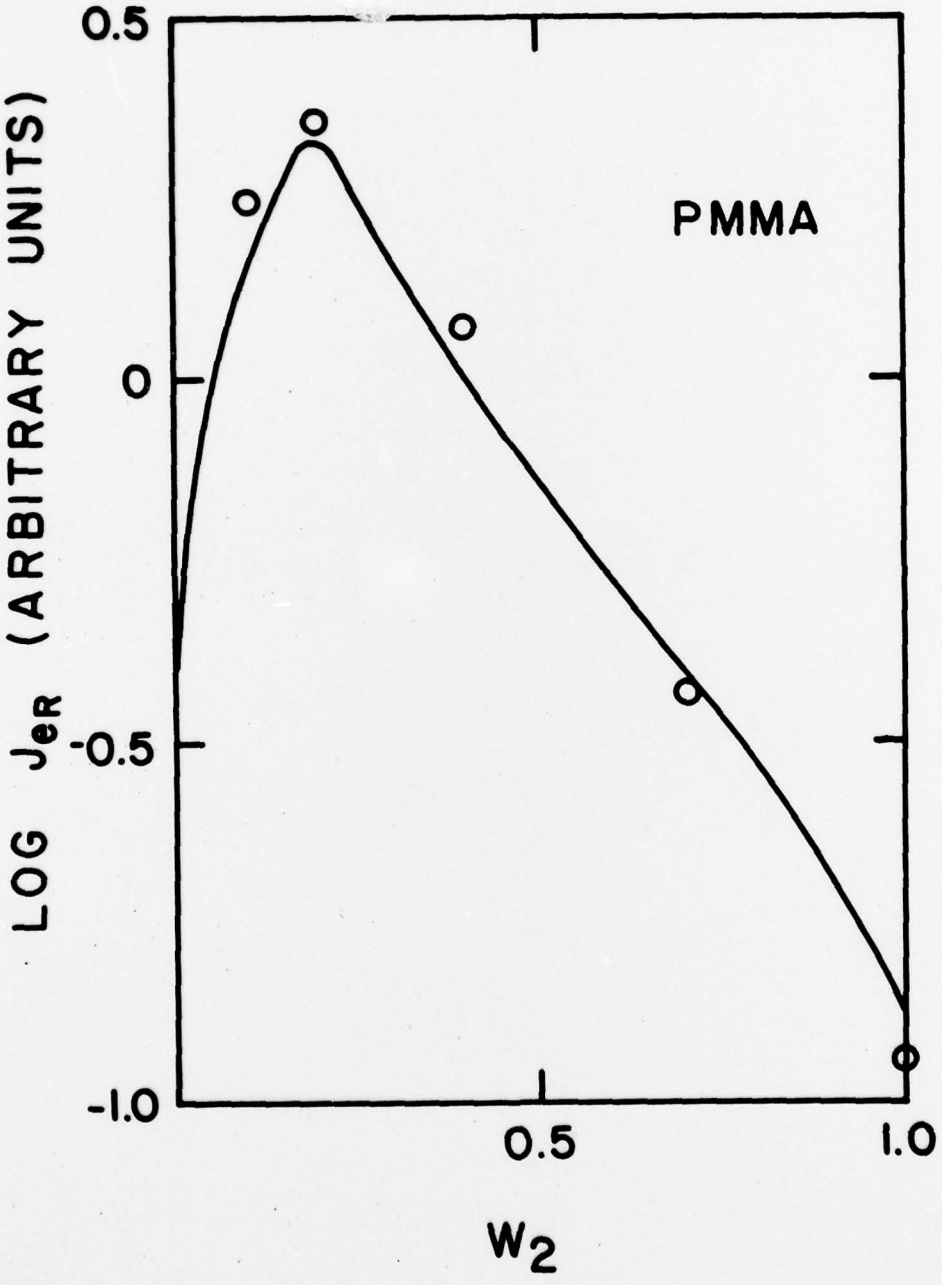
0.5
0
-0.5
-1.0
0.5
1.0
PMMA
LOG J_{eR} (ARBITRARY UNITS)
W_2

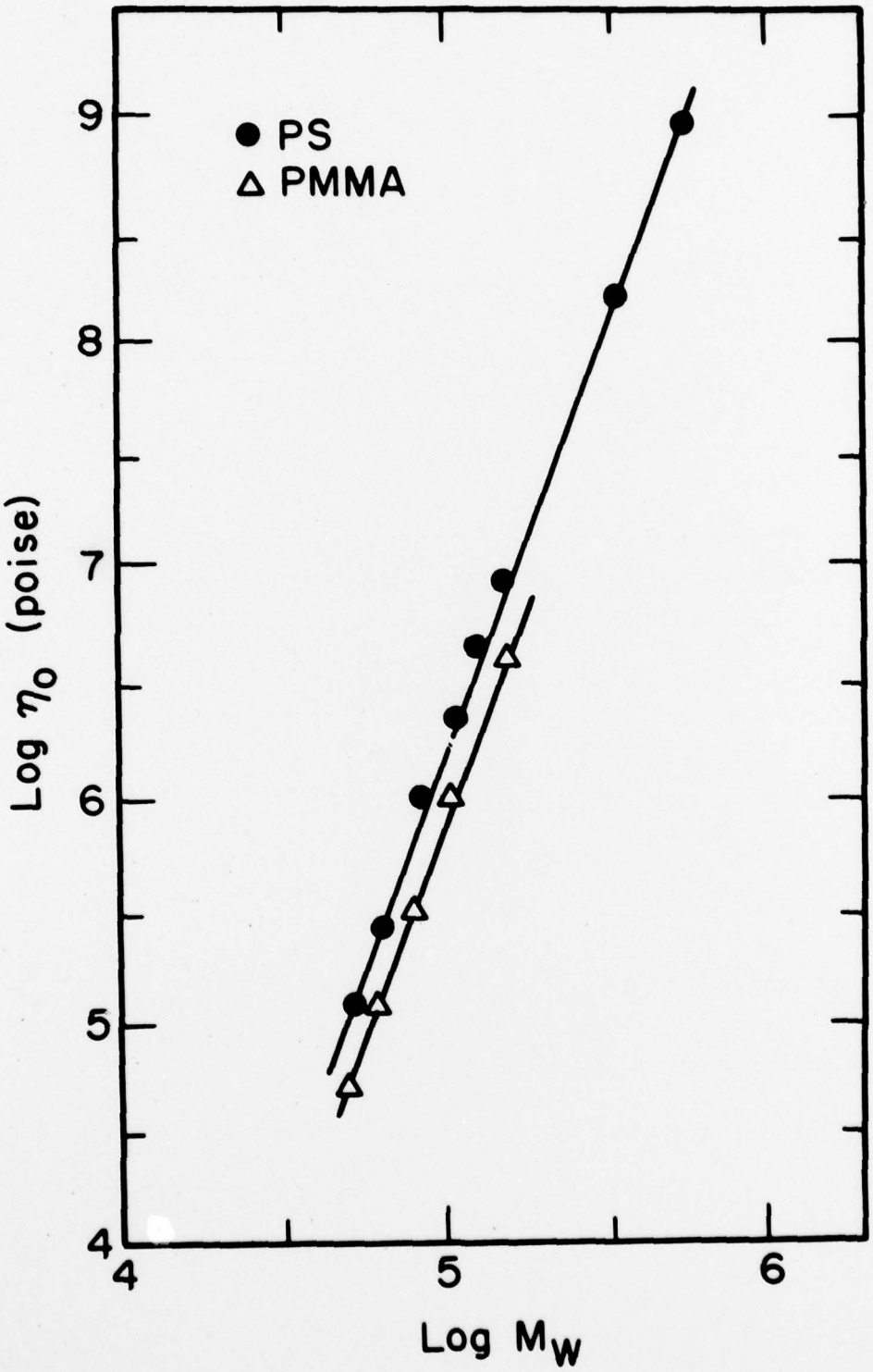
● PS
△ PMMA
9
8
7
6
5
4
4
5
6
Log η_o (poise)
Log M_W

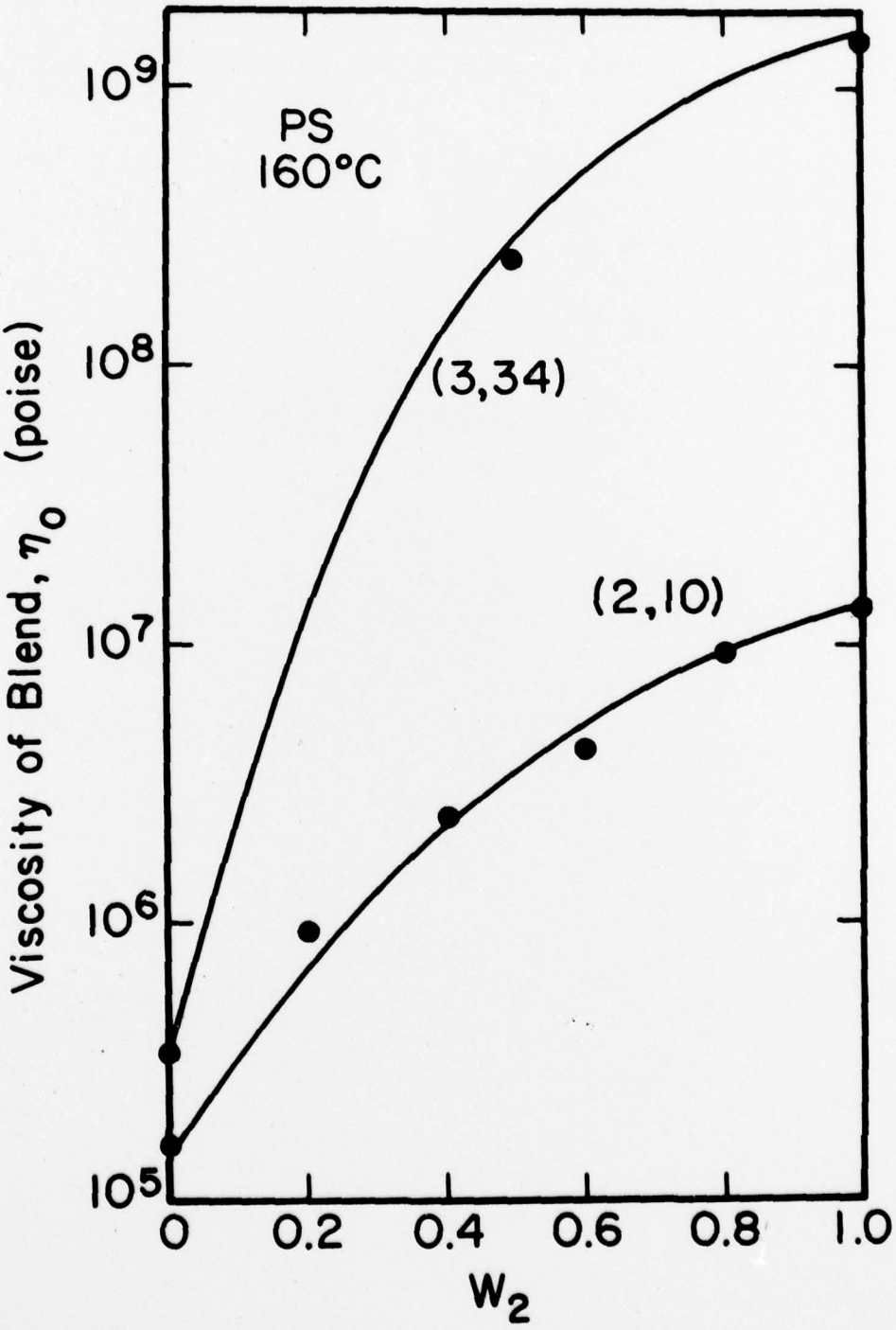
PS
160°C
(3,34)
(2,10)
Viscosity of Blend, η_o (poise)
10^9
10^8
10^7
10^6
10^5
0
0.2
0.4
0.6
0.8
1.0
W_2

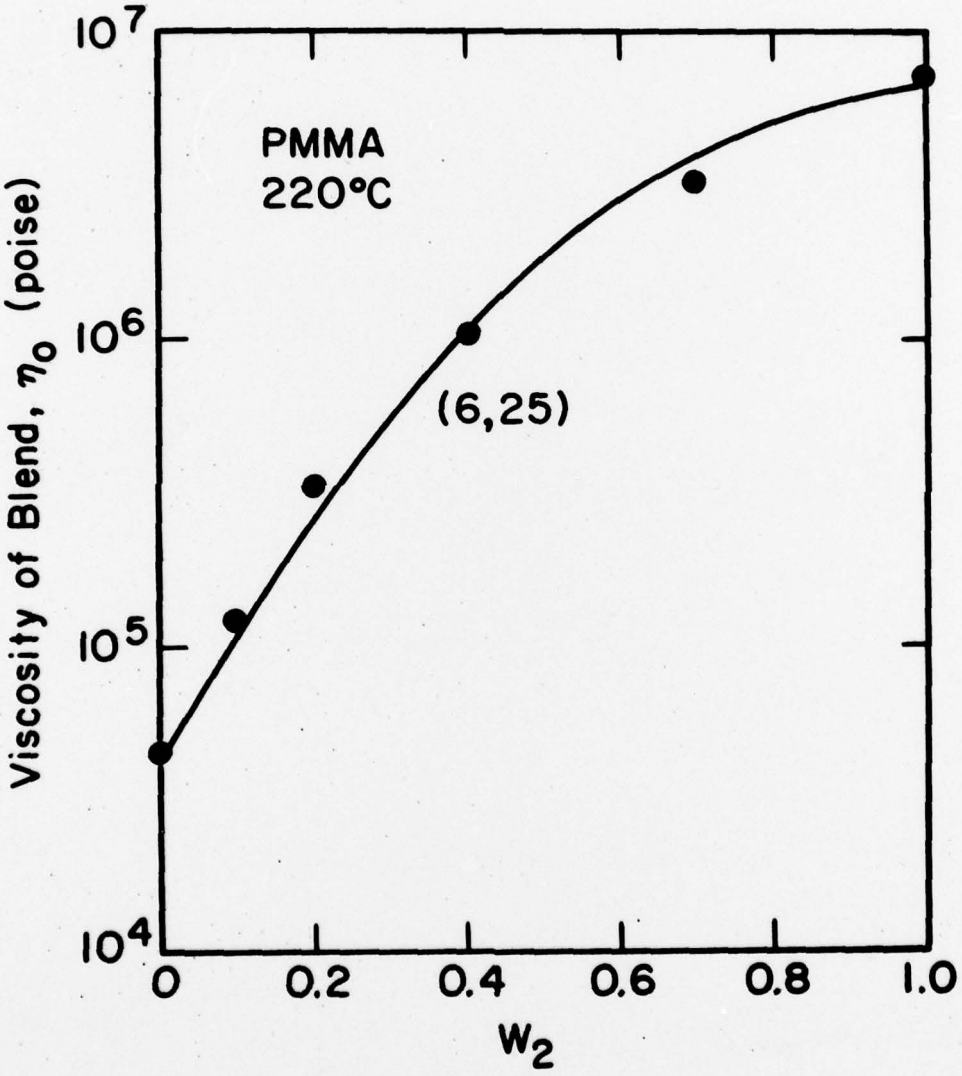
PMMA
220°C
(6,25)
Viscosity of Blend, η_0 (poise)
10^7
10^6
10^5
10^4
0
0.2
0.4
0.6
0.8
1.0
W_2

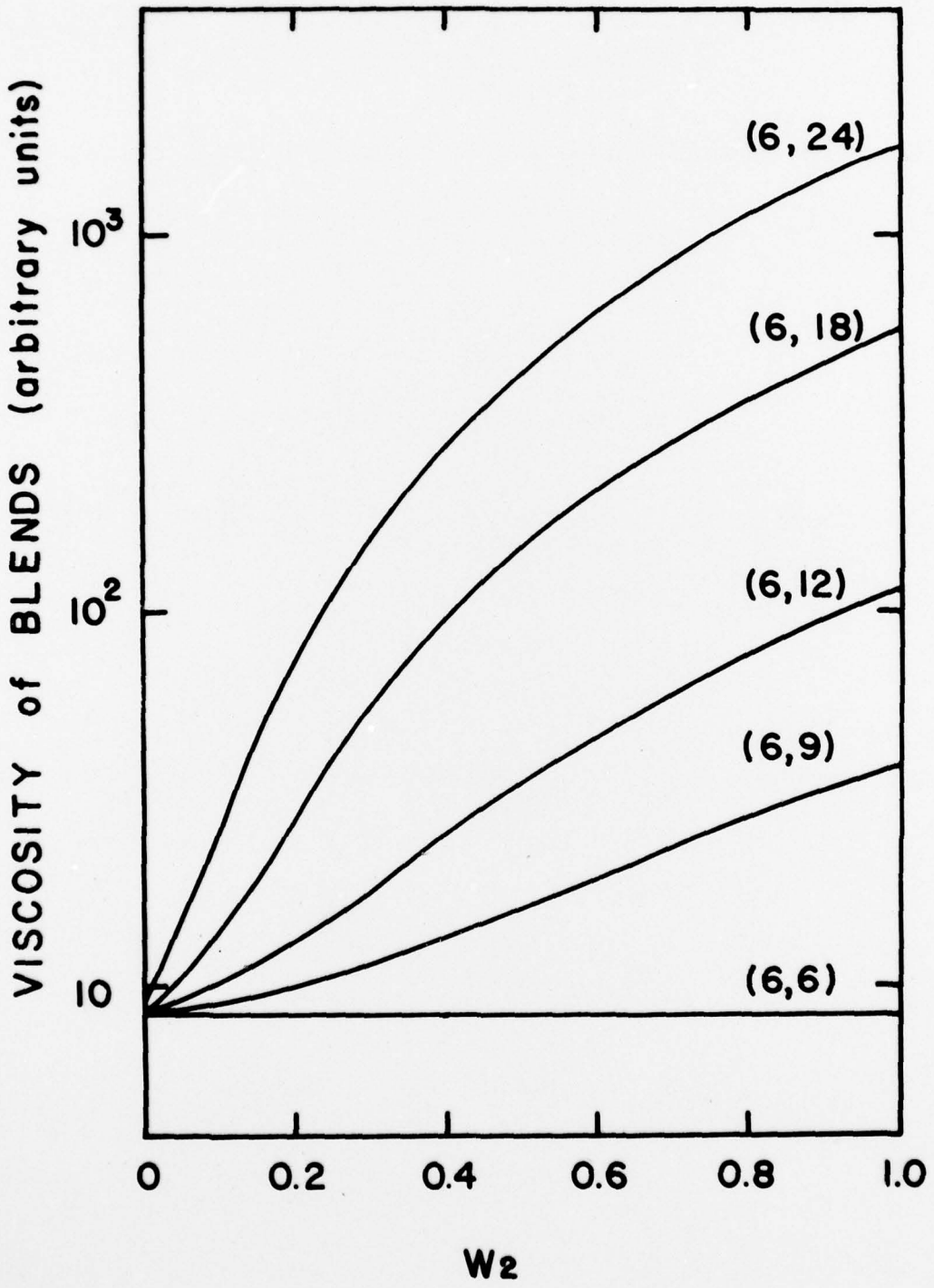
VISCOSITY of BLENDS (arbitrary units)
10^3
10^2
10
(6, 24)
(6, 18)
(6,12)
(6,9)
(6,6)
0
0.2
0.4
0.6
0.8
1.0
W2

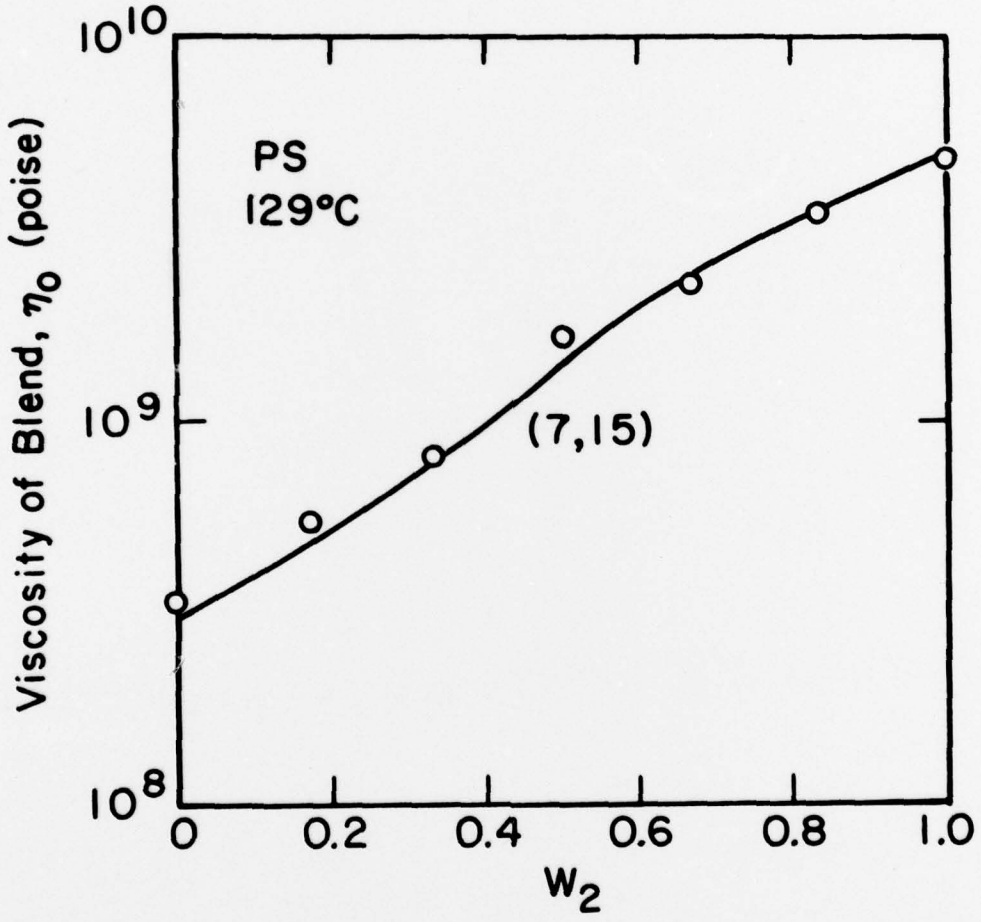
Viscosity of Blend, η_o (poise)
10^{10}
10^9
10^8
PS
129°C
(7,15)
0
0.2
0.4
0.6
0.8
1.0
W_2

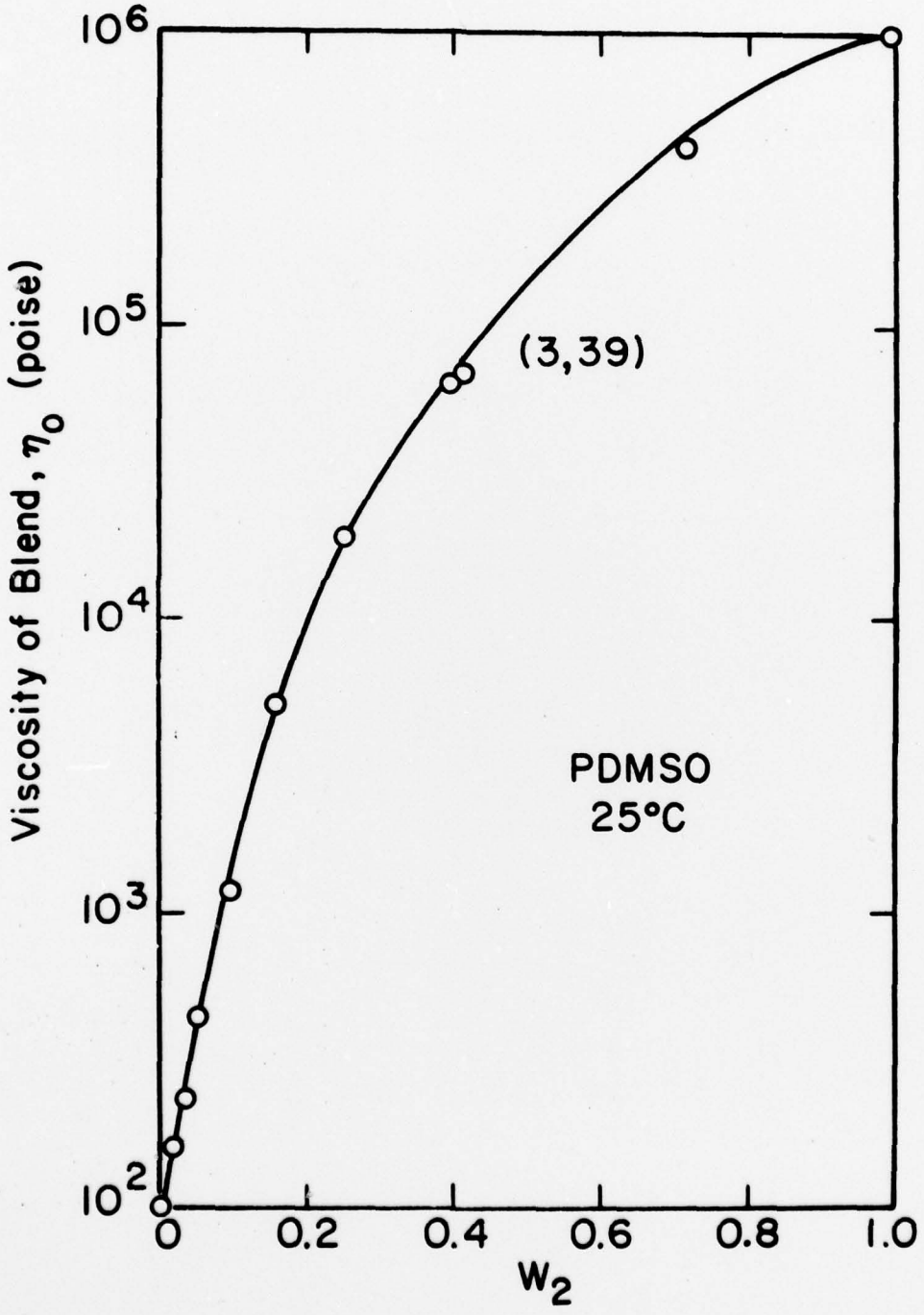
Viscosity of Blend, η_0 (poise)
10^6
10^5
10^4
10^3
10^2
(3,39)
PDMSO
25°C
0
0.2
0.4
0.6
0.8
1.0
W_2